Mutagenic and Inhibitory Effects of Ribavirin on Hepatitis C Virus RNA Polymerase†

Nam V. Vo,‡ Kung-Chia Young,‡,§ and Michael M. C. Lai*,‡,||

Department of Molecular Microbiology and Immunology and Howard Hughes Medical Institute, University of Southern California School of Medicine, Los Angeles, California 90033-1054, and Department of Medical Technology, College of Medicine, National Cheng Kung University, Tainan, Taiwan

Received March 24, 2003; Revised Manuscript Received June 10, 2003

ABSTRACT: Crotty *et al*. recently proposed the primary antiviral action of ribavirin to be that of a potent RNA mutagen [Crotty, S., Maag, D., Arnold, J. J., Zhong, W., Lau, J. Y., Hong, Z., Andino, R., and Cameron, C. E. (2000) *Nat. Med. 6*, 1375−1379]. Here we investigate the effect of ribavirin triphosphate (RTP) on RNA synthesis catalyzed by a full-length hepatitis C virus (HCV) RNA polymerase *in vitro*. HCV polymerase can use RTP as a nucleotide substrate in a template-dependent manner, incorporating it opposite a pyrimidine (C or U) template residue, but not a purine (A or G). Kinetic analysis revealed that incorporation of ribavirin monophosphate (RMP) across from C is 3 times more efficient catalytically than that across from U, as determined by the k_{cat}/K_m parameter. The efficiency of RMP incorporation, however, is 50−100 fold lower than that of the natural NMP. RMP incorporation does not lead to termination of RNA chain synthesis, as evidenced by the ability of the polymerase to extend its RNA product many nucleotides beyond the site of RMP incorporation. However, multiple-RMP incorporation at low GTP concentrations induced the formation of stalled elongation complexes, particularly at the template region containing consecutive C residues. Most, but not all, such elongation blocks can be relieved by the re-addition of GTP. When ribavirin is present in the RNA template, pyrimidine (but neither purine nor ribavirin) monophosphate is incorporated opposite ribavirin, but at an exceedingly low catalytic efficiency (200−3000-fold lower) compared to the efficiencies of those templated by A or G. Consequently, the level of RNA synthesis on a ribavirin-containing template is significantly reduced. These findings suggest that ribavirin not only is mutagenic but also interferes with HCV polymerase-mediated RNA synthesis.

Hepatitis C virus (HCV)[1] is a major human pathogen, causing both acute and chronic hepatitis, which often leads to liver cirrhosis and hepatocellular carcinoma. HCV possesses a (+)-strand RNA genome of ∼9.5 kb, within which resides a single open reading frame (ORF) encoding a polyprotein of ∼3000 amino acids (*2*, *3*). The key replicative enzyme of this virus is NS5B, a 66 kDa membrane-associated protein derived from the C-terminal end of the polyprotein (*4*−*8*). The current primary treatment of HCV infection involves the combination of interferon-α (IFN-α) and ribavirin, which give rise to significantly more viral clearance in patients than IFN-α monotherapy, confirming the antiviral activity of ribavirin (*9*, *10*). Developed in 1972, ribavirin is a nucleoside analogue, 1-β-D-ribofuranosyl-1,2,4-triazole-3-carboxamide, that exhibits antiviral activity against a variety of RNA and DNA viruses (*11*). In addition to its use in treating HCV infection, ribavirin monotherapy is the current clinical treatment for Lassa fever virus (*12*) and severe respiratory syncytial virus infection (*13*, *14*). The mechanism of the antiviral effects of ribavirin on HCV is not well-understood. After cellular uptake, ribavirin is metabolically converted into mono-, di-, and triphosphate forms (*15*, *16*). Until recently, it was believed that ribavirin monophosphate (RMP) suppresses viral replication through a nonspecific pathway, i.e., by reducing the intracellular GTP pool via its inhibition of inosine monophosphate dehydrogenase (IMPDH) (*17*). The decrease in the level of intracellular GTP is thought to somehow adversely affect viral protein and RNA synthesis.

Mounting evidence indicates that the primary antiviral effect of ribavirin is not through the reduction of the GTP pool by RMP inhibition of IMPDH (*18*). For instance, ribavirin and mycophenolic acid are both potent IMPDH inhibitors, but only ribavirin exhibits antiviral activity against the GB virus (*19*), the closest known relative to HCV. In addition, studies using the influenza virus model system demonstrated that only a modest antiviral effect (∼2-fold)

† This work was partially supported by National Institutes of Health Grant AI 47348. M.M.C.L. is an Investigator of the Howard Hughes Medical Institute.

* To whom correspondence should be addressed: 2011 Zonal Ave., HMR-401, Los Angeles, CA 90033-1054. Phone: (323) 442-1748. Fax: (323) 442-1721. E-mail: michlai@hsc.usc.edu.

‡ Department of Molecular Microbiology and Immunology, University of Southern California School of Medicine.

§ National Cheng Kung University.

|| Howard Hughes Medical Institute, University of Southern California School of Medicine.

[1] Abbreviations: RdRp, RNA-dependent RNA polymerase; DdRp, DNA-dependent RNA polymerase; RTP, ribavirin triphosphate; RMP, ribavirin monophosphate; IMPDH, inosine monophosphate dehydrogenase; HCV, hepatitis C virus.

10.1021/bi0344681 CCC: $25.00
Published on Web 08/14/2003

was obtained at ≤25 μM ribavirin, whereas 25 μM is the saturating ribavirin concentration that causes maximal intracellular GTP reduction (~40%) (*20*). However, the highest antiviral activity (~20-fold) was achieved with ribavirin above 25 μM, suggesting that some other antiviral mechanism besides GTP pool reduction is responsible for the observed antiviral effect. Effects of ribavirin on cellular processes other than IMPDH have been reported, such as RMP inhibition of guanylyltransferase activity (*21*) and viral transcription (*22*).

Recent studies have suggested that the major mechanism of ribavirin action is through lethal mutagenesis of the viral RNA genome. Using the poliovirus model system, Crotty *et al*. showed that ribavirin increased the mutation frequency of this viral genome in a dose-dependent manner (*1*, *23*). More importantly, high doses of ribavirin led to a phenomenon called "error catastrophe", in which most viruses became lethally mutated, resulting in a more than 95% reduction in the specific infectivity of viral RNA. Similarly, ribavirin treatment of hepatocytes infected with GB virus B resulted in a drastic reduction of the specific infectivity of viral RNA (*19*). Higher mutation frequencies associated with ribavirin treatment have also been reported for HCV (*24*) and Hantaan virus systems (*25*) *in vivo*.

In vitro studies showed that the poliovirus polymerase can incorporate ribavirin triphosphate as a nucleotide analogue of either ATP or GTP, and ribavirin itself can serve as a template base for incorporation of cytidine or uridine with equal efficiency (*1*). Such promiscuous incorporation explains the observed G-to-A and C-to-U transition mutations. Using a modified HCV polymerase lacking the β-loop and the 21-amino acid hydrophobic C-terminus, Magg and coworkers reported incorporation of RMP opposite C and U by this enzyme, and this enzyme incorporated cytidine and uridine across from R on an RNA template with equivalent efficiencies (*26*). The same study also reported that the presence of ribavirin in the RNA template partially blocked RNA elongation. However, these authors only presented the k_{pol} and K_d kinetic parameters of nucleoside incorporation without providing any direct evidence for template-specific incorporation of RMP. Thus, it is not clear from these studies whether RMP incorporation can occur randomly opposite any of the four templating bases or, more strictly, the pyrimidines, nor is it known if RMP incorporation occurs only at the 3′ end of the RNA template through the nucleotidyl transferase activities reported previously (*27*). Moreover, it is not known whether the absence of the β-loop and the 21-amino acid hydrophobic C-terminus can affect nucleotide selection of the HCV polymerase. In this study, we investigated the direct *in vitro* effect of ribavirin triphosphate on a full-length HCV polymerase. Our results demonstrated that HCV polymerase can incorporate RMP into its RNA product in a template-specific manner, across pyrimidine but not purine residues. We found that multiple-RMP incorporation at low GTP levels led to the formation of stalled elongation complexes, and the presence of ribavirin on the RNA template severely reduced the extent of RNA synthesis. Thus, the anti-HCV effect of ribavirin is mediated through its polymerase both by introducing mutations and by inhibiting RNA synthesis.

EXPERIMENTAL PROCEDURES

Materials. Reagents were purchased from the following sources: [α-^{32}P]NTP and [γ-^{32}P]GTP from NEN, HPLC-grade nucleoside triphosphates and glycogen from Pharmacia, RNase A, RNase T1, and T7 MEGAscript In Vitro Transcription Kit from Ambion, betaine from Sigma, oligonucleotides from the University of Southern California Norris Microchemical Core Facility, ribavirin triphosphate from GenaBioscience, Moraveck, and Rib10 RNA oligonucleotide from Dharmacon.

Purification of HCV NS5B. The recombinant NS5B derived from NS5B NIH1b strain was purified from the DH5α *Escherichia coli* strain by the method of Vo *et al*. (*28*). This full-length NS5B protein contains a tag of six histidines at the N-terminus of the protein for affinity chromatographic purification.

Preparation of RNA Templates. Large quantities of RNA templates were made from runoff transcription reactions using the T7 promoter-containing PCR DNA templates and reagents from Ambion's T7 MEGAscript In Vitro Transcription Kit. These RNA templates were purified from a 7.5% denaturing polyacrylamide gel (PAG). The RNA concentration was determined spectrophotometrically. The PCR DNA templates containing the T7 promoter were prepared using the oligonucleotide T7-TMOAR/D (3′-CCTCACCCCAC-CCACCACCCCGGGCCCAAACAA CAACAAACAAGTC-GACCACCACTCGCGGGATATCACTCAGCATAAT-5′) and a combination of an upstream primer (5′-GGAGTGGGG-TGGGTGGTGGG-3′) and a downstream primer (3′-GTC-GACCACCACTCGCGGGATATCACTCAGCA-TAATCTTAAGG-5′). The core T7 promoter sequence is underlined. Transcription from this PCR DNA using the T7 RNA polymerase yields a 62-nucleotide runoff RNA product, which serves as a template for the NS5B RdRP assay. To make a complementary RNA, we synthesized a PCR product that contained the T7 promoter at the opposite end of the transcribed sequence; we also used this T7-PCR DNA template to produce the [γ-^{32}P]GGA RNA primer using [γ-^{32}P]GTP and ATP, and purified it by 23% denaturing PAGE.

NS5B RNA-Dependent RNA Polymerase (RdRp) Assay. In a standard 20 μL reaction volume, 2 μM NS5B was incubated with 2.5 μM RNA template and 100 μM NTP in NS5B transcription buffer [50 mM HEPES (pH 7.3), 5 mM $MgCl_2$, 10 mM β-mercaptoethanol, 50 mM KCl, 100 mM betaine, 0.05% Tween 20, and 10 μg/mL acetylated bovine serum albumin]. For *de novo* RNA synthesis, [γ-^{32}P]GTP (0.1 mM, ~10^4 cpm/pmol) was used to terminally label the RNA product. For primer-dependent RNA synthesis, the [γ-^{32}P]GGA primer (10 μM, 1000−2000 cpm/pmol) was used. The reaction mixtures were incubated at 30 °C for a desired period of time; the reactions were stopped by phenol extraction, and the RNA products were precipitated using ethanol in the presence of 0.5 mg/mL glycogen as a carrier. The precipitated pellet was dried down and dissolved in FLB {formamide loading buffer [89 mM Tris-borate (pH 8.3), 2.5 mM EDTA, 0.05% xylene cyanol and bromophenol blue dyes, 10 mM EDTA, and 80% freshly deionized formamide]}. The dissolved RNA samples were heated at 100 °C for 3 min, and resolved on a 23% (38:2 acrylamide: bisacrylamide) polyacrylamide gel containing 8 M urea. Gel

electrophoresis was performed using TBE buffer [89 mM Tris-borate (pH 8.3) and 2.5 mM EDTA]. After electrophoresis, the gels were directly exposed to a phosphorimager screen and scanned using a Molecular Dynamic PhosphorImager. To obtain a conversion factor between phosphorimager counts and (femto)moles of RNA, known amounts of the labeling nucleotide solution of a given specific activity were spotted on the same gel and exposed to the phosphorimager screen.

Single-Nucleotide Incorporation (SNI) Assay. NS5B (2 μM) was preincubated with the 2.5 μM RNA template and 10 μM [γ-^{32}P]GGA primer in a 20 μL reaction volume. The reaction was initiated by adding the next nucleotide at the desired concentration and the mixture incubated at 30 °C for varying lengths of time as specified. GGAA, GGAG, GGAC, and GGAU RNA markers were made using the parental T7-DNA PCR templates, T7 RNA polymerase, and [γ-^{32}P]GGA primer. The RNA products were analyzed by denaturing 23% PAGE and quantified as described above.

Assay for K_m and k_{cat}. Using the SNI assay, the initial steady-state synthesis rate of each of the GGAA, GGAG, GGAC, and GGAU RNA products was determined at various nucleotide concentrations. For normal NTP and RNA template, the kinetics of initial RNA synthesis occurred at a constant rate up to 1.5 min. For C- or U-templated RMP incorporation, initial synthesis showed a constant rate for the first 5 or 20 min of the reaction, respectively. For R-templated CMP or UMP incorporation, initial steady-state synthesis occurred for at least 30 min. Double-reciprocal plots of 1/rate and 1/nucleotide concentration were made for each combination of template and nucleotide. The k_{cat} and K_m kinetic parameters were determined by a direct fit of the data to the Michaelis−Menten equation. One standard deviation was included for each K_m and k_{cat} determination from three to five independent experiments.

RNAse Cleavage Analysis of the RNA Product. The 62-nucleotide RNA was 5′-terminally labeled using T7 RNA polymerase and [γ-^{32}P]GTP. The end-labeled RNA product was digested in a 10 μL reaction volume by three separate ribonucleases for 1 min at 30 °C: RNase A (0.01 μg/mL), RNase T1 (10 units/μL), and RNase Cl3 (10 units/mL). The reactions were stopped by phenol extraction, and the RNA products were recovered by ethanol precipitation using glycogen as a carrier. Piperidine ladders of 5′-end-labeled RNA were generated by incubating 1 pmol of 5′-end-labeled RNA with carrier yeast tRNA (0.3 mg/mL) in a volume of 20 μL with 1% piperidine at 92 °C for 2 min. The digested RNA products were resolved on a denaturing 8 M urea-containing 23% polyacrylamide gel.

RESULTS

Rationale. Our objective in these studies was to investigate whether RTP directly affects the RdRP activity of the HCV RNA polymerase NS5B. We devised an *in vitro* assay system that allows us to quantitatively examine the RdRP activity of the purified full-length HCV NS5B in the presence or absence of RTP. A 62-nucleotide synthetic RNA with minimal RNA secondary structure was used as a template (Figure 1A). Using this template, HCV NS5B generated a full-length complementary RNA product through either *de novo* RNA synthesis with [γ-^{32}P]GTP (Figure 1B, lanes 2−5) or primer-dependent synthesis using [γ-^{32}P]GGA as a primer (Figure 1B, lanes 6−9). The RNA product comigrated with the *in vitro* transcript synthesized from a corresponding DNA template by T7 RNA polymerase (lane 1). At 100 μM [γ-^{32}P]-GTP, HCV NS5B carried out *de novo* synthesis less efficiently than primer-dependent synthesis (10 μM [γ-^{32}P]-GGA primer) (Figure 1C). However, at higher GTP concentrations (1−5 mM), *de novo* synthesis was more efficient than primer-dependent synthesis at all the concentrations that were tested (data not shown).

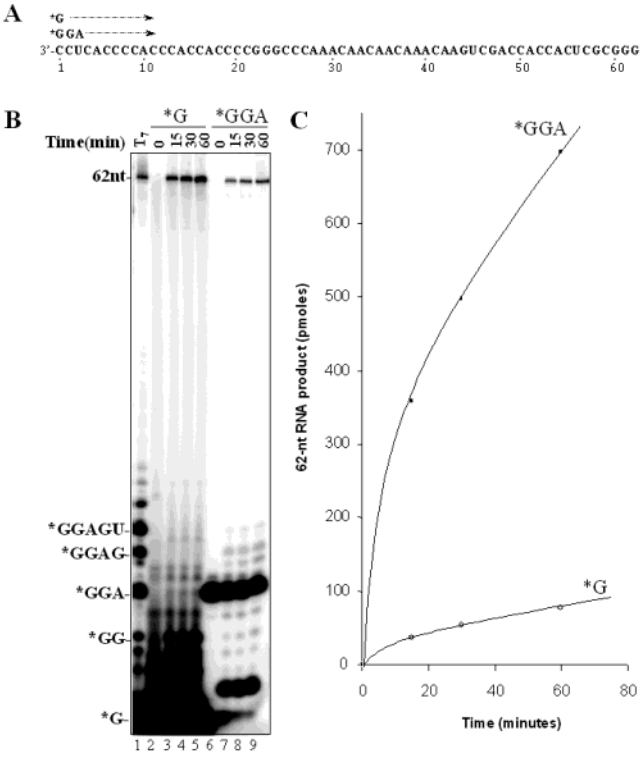

FIGURE 1: Outline of the *in vitro* RdRp assay used in these studies. (A) Sequence of the RNA template and primer that were used. (B) Gel analysis of RNA products from *de novo* and primer-dependent syntheses: lane 1, RNA marker synthesized by T7 RNA polymerase (abortive ladder is shown); lanes 2−5, time course of *de novo* synthesis; and lanes 6−9, time course of GGA primer-dependent RNA synthesis. (C) Kinetic profile of the synthesis of the full-length 62-nucleotide RNA.

This *in vitro* assay system contains several significant features. The use of [γ-^{32}P]GTP instead of [α-^{32}P]NTP allows for detection of only *de novo* RNA products and eliminates the interference from the terminal nucleotidyl transferase (TNT) activity of NS5B (*27*). The use of [γ-^{32}P]GTP to terminally label the RNA products also allows for simple and quantitative measurement of the amount of RNA produced. NS5B-mediated RNA synthesis in this assay produces a single well-defined full-length RNA product and a negligible amount of the intermediate products, which greatly simplified the interpretation of our results. Finally, this template allows us to study template-specific incorporation of a nucleotide by using a combination of a primer and a limited subset of NTP (see below).

RTP Has Only a Minor Inhibitory Effect on the Overall de Novo RNA Synthesis by NS5B. We first determined whether RTP affects the overall RNA synthesis by NS5B. The presence of RTP had no significant effect on the overall RNA synthesis even when the RTP concentration was 10-

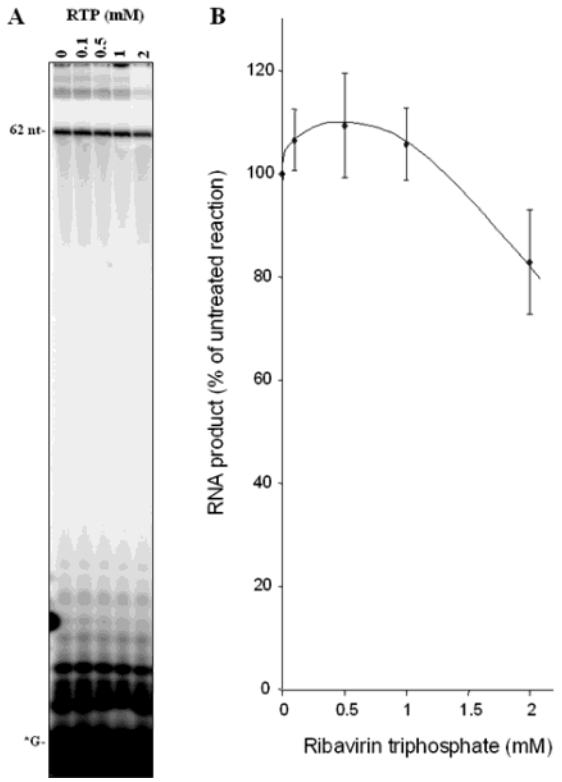

FIGURE 2: Effect of RTP on RNA synthesis by HCV polymerase. (A) Gel analysis of RNA products synthesized using 0.1 mM NTP in the presence of increasing RTP concentrations (from 0 to 2 mM). (B) Quantitation of the effect of RTP on 62-nucleotide RNA synthesis. One standard deviation is plotted from three independent experiments.

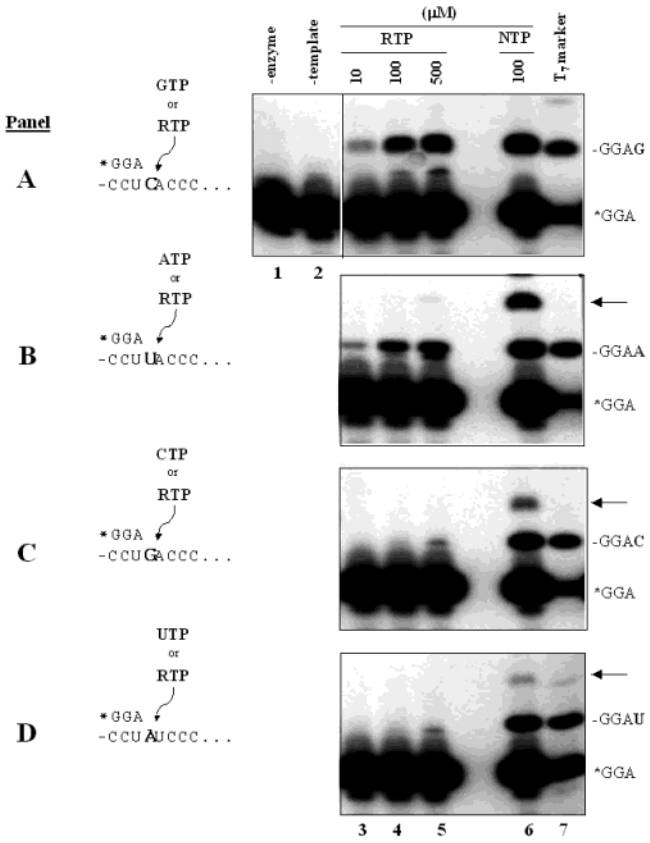

FIGURE 3: Template-specific incorporation of RTP opposite various template nucleosides. The 62-nucleotide template and GGA primer sequence combination that was used is shown at the left. In lanes 3−5, RTP was present at 10, 100, and 500 μM, respectively. In lane 6 is shown NS5B-mediated synthesis using a single NTP (100 μM) complementary to the fourth nucleoside of the template. In lane 7 is an RNA marker synthesized by T7 RNA polymerase. Lane 1 is without HCV polymerase. Lane 2 is without template RNA. Panels A−D show different combinations of the template and NTP as specified. Arrows denote terminal addition products or read-through products due to either misincorporation or the presence of traced contaminants of other NTPs.

fold higher than those of the normal NTP (1 mM RTP *vs* 0.1 mM NTP) (Figure 2); similar results were observed when ribavirin was used in place of RTP (data not shown). In fact, slight enhancement of RNA synthesis was noted at lower RTP concentrations. Only at a 20-fold excess of RTP was a slight inhibition of RNA synthesis observed. Thus, RTP does not significantly affect the overall RNA synthesis by HCV NS5B.

NS5B Incorporates RMP in a Template-Dependent Manner Across from a Pyrimidine Residue. To test whether RTP has other effects on HCV RNA polymerase, we examined the ability of NS5B to incorporate RMP specifically into the nascent RNA product. A 5′-end-labeled GGA oligonucleotide was used as an RNA primer on various templates that differ at the fourth nucleotide from the 3′ terminus. Because of the sequence design, addition of the next complementary NTP only would result in a four-nucleotide RNA product (Figure 3). As expected, HCV polymerase incorporated each of its four natural NTPs in a template-specific manner (Figure 3, lane 6 in panels A−D), yielding a four-nucleotide product, which comigrated with the control RNAs produced by T7 RNA polymerase from the corresponding DNA templates (Figure 3, lane 7). However, when ATP, CTP, or UTP was used in the reaction, small amounts of longer RNA products were also produced, most likely through terminal addition or traced contaminants of other NTP (arrows in Figure 3, panels B and C, lane 6).

When RTP was used in place of the natural NTP, the four-nucleotide product was seen only on the template containing C or U at the fourth position (Figure 3, lanes 3−5 of panels A and B), but not A or G residues (Figure 3, lanes 3−5 of panels C and D). The extent of RMP incorporation was proportionate to its concentration (Figure 3, lanes 3−5 in panels A and B). C-Templated incorporation of RMP was slightly more efficient than U-templated incorporation (Figure 3, compare lanes 3−5 of panels A and B). In the absence of a template, NS5B did not add RMP onto the 3′ end of the GGA primer (panel A, lane 2). These results showed that RMP mimics a purine nucleotide, consistent with the molecular modeling which shows that RTP with the pseudobase in the anti conformation base pairs with cytidine or uridine through two hydrogen bonds (*1*). We also tested for possible RMP incorporation by T7 DNA-dependent RNA polymerase (DdRP), but such a reaction did not occur (data not shown), suggesting that RMP incorporation might be restricted to certain viral RdRPs.

Efficiency of RMP Incorporation by the HCV Polymerase. To examine how efficiently HCV polymerase incorporates RMP as compared to the natural NMP, we next determined the kinetic parameters of incorporation of RMP and each of the four NMPs. The incorporation of RMP across from C revealed biphasic kinetics, an initial burst phase followed by a slower second phase, similar to GMP incorporation (Figure 4). The incorporation in the second phase remained

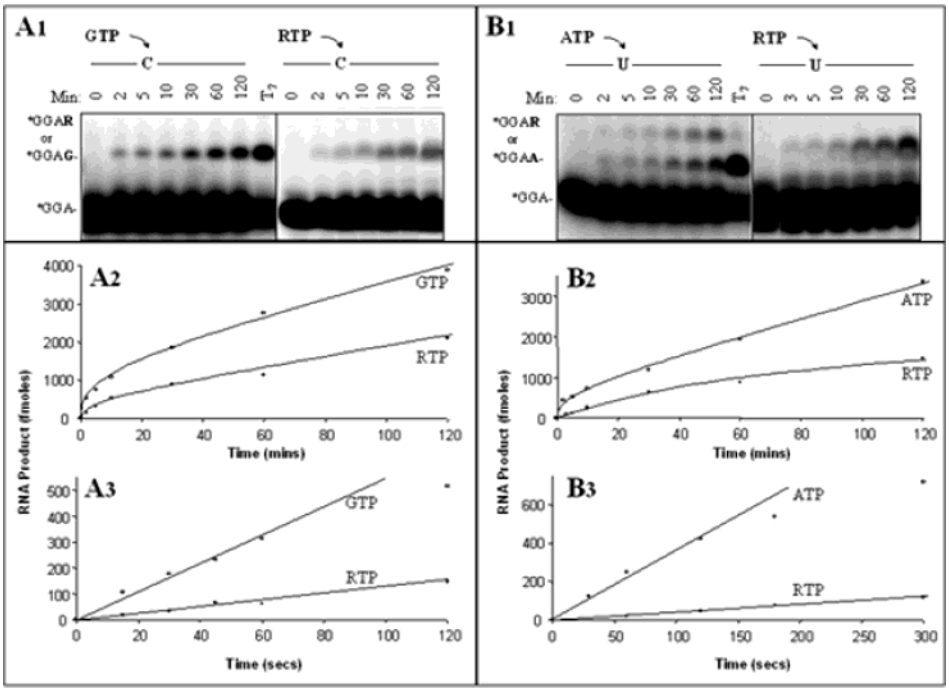

FIGURE 4: Kinetics of incorporation of RTP templated by C or U. (A1) Gel analysis of time course incorporation of GTP or RTP opposite C using 0.1 mM GTP or RTP. The GGAG RNA marker synthesized by T7 RNA polymerase is included in lane T7. (A2) Plots of kinetics of GTP and RTP incorporation from 0 to 120 min. (A3) Plots of initial kinetics of GTP and RTP incorporation from 0 to 120 s. The *Y*-axis gives the amount of four-nucleotide RNA in femtomoles. (B1−B3) Same as A1−A3, respectively, except that an RNA template containing a U at the fourth position from the 3′ end was used.

constant over the course of 2 h (Figure 4, panel A2), indicative of the ability of the HCV polymerase to recycle continuously under this reaction condition. However, the slower kinetics of synthesis during the second phase also suggested that a fraction of the NS5B enzyme failed to recycle or became inactivated after the completion of the initial phase of the reaction. Such a phenomenon has been reported for *E. coli* DNA-dependent RNA polymerase (*29*, *30*). RMP incorporation across from C was significantly slower than GMP incorporation, but both shared similar kinetic curves. The initial burst phase for GMP incorporation remained linear for ~1 min, while that for RMP lasted for up to 5 min (Figure 4, panel A3, and data not shown for the 5 min time point). Incorporation of AMP and RMP opposite U (Figure 4, panels B1−B3) displayed kinetics similar to those of incorporation of GMP and RMP opposite C, respectively. The nucleotide incorporation rate during the initial phase of synthesis was used subsequently for kinetic comparison to avoid the complication of possible inactivated or unrecycled enzyme fraction formed during the second phase. At 0.1 mM nucleotide substrate, a saturated concentration for normal NTP, NS5B incorporates 311 fmol GMP min^{-1} (μg of NS5B)$^{-1}$, a rate 5 times faster than that for RMP [61 fmol min^{-1} (μg of NS5B)$^{-1}$] (Table 1). Similarly, NS5B incorporates 302 fmol of AMP min^{-1} (μg of NS5B)$^{-1}$, a rate 15 times faster than that for RMP [21 fmol min^{-1} (μg of NS5B)$^{-1}$]. Even at the saturating concentration of 0.5 mM RTP, RMP incorporation (~150 fmol/min) across C and U still occurred only half as fast as that of its GMP and AMP counterparts (~300 fmol/min).

The slower RMP kinetics of incorporation could reflect the lower affinity of NS5B for RTP with respect to the natural NTP. We tested this hypothesis by measuring the K_m values for the incorporation of RTP and each of the four

Table 1: Initial Rates of Single-Nucleotide Incorporation

		rate [fmol min^{-1} (mg of NS5B)$^{-1}$]	
nucleotide	template	100 μM[a]	500 μM[a]
ATP	U	302 ± 63	302 ± 63
RTP	U	21 ± 1	145 ± 7
GTP	C	311 ± 14	311 ± 14
RTP	C	61 ± 6	150 ± 14
CTP	G	317 ± 11	317 ± 11
CTP	R	8 ± 3	77 ± 7
UTP	A	184 ± 28	184 ± 28
UTP	R	3.8 ± 0.1	41 ± 4

[a] Concentration of the NTP or RTP substrate.

NTPs to estimate their relative affinities for the NS5B replicating complex. The initial rates of steady-state synthesis were determined at various concentrations for each of the four natural NTPs and RTP using the appropriate templates. Double-reciprocal plots of rate and NTP concentration were made, and K_m and k_{cat} values for each nucleotide were determined from the direct fit of the data to the Michaelis−Menten equation (Table 2).

When templated by C, HCV NS5B incorporated GTP and RTP with K_m values of ~5 and ~63 μM, respectively (Table 2). On the basis of the K_m/k_{cat} ratio, which is a measure of the catalytic efficiency and enzyme specificity, HCV polymerase incorporates GMP ~50-fold more efficiently than RMP (Table 2). We also found that RTP competitively inhibited GMP incorporation with a K_i of 42 mM, but RTP did not interfere with UMP incorporation (data not shown). This could be due to the fact that RTP is a nucleotide analogue with strict template specificity, being incorporated across pyrimidines but not A or G, and therefore does not compete with UTP. These results also demonstrated that there is no additional effect, such as allosteric inhibition, on HCV polymerase activity.

Table 2: Kinetic Parameters for Incorporation of Different Nucleotides

nucleotide	template	K_m (μM)	k_{cat}[a] ($\times 10^3$ h^{-1})	k_{cat}/K_m[a] ($\times 10^4$ μM^{-1} h^{-3})
ATP	U	4.4 ± 1.2	1.02 ± 0.2	2.3
RTP	U	92 ± 1.2	0.17 ± 0.01	0.02
GTP	C	4.9 ± 1.3	1.3 ± 0.1	2.7
RTP	C	63 ± 6	0.36 ± 0.5	0.06
CTP	G	3.5 ± 0.1	1.29 ± 0.3	3.7
CTP	R	23 ± 3	0.038 ± 0.001	0.02
UTP	A	0.6 ± 0.1	0.66 ± 0.05	11
UTP	R	76 ± 6	0.027 ± 0.001	0.004

[a] k_{cat} values multiplied by 10^{-3} and K_m values multiplied by 10^{-4}. For example, the k_{cat} of AMP incorporation is 1.02×10^{-3}, and the k_{cat}/K_m is 2.3×10^{-4}.

The K_m of U-templated RMP incorporation is 92 μM, while that of AMP incorporation is 4.4 μM. Their k_{cat}/K_m values revealed that RMP incorporation is more than 100-fold less efficient than that of AMP opposite U. Thus, RMP incorporation by the HCV polymerase is much less efficient than incorporation of the natural AMP or GMP. It should be noted that AMP incorporation in our SNI assay was complicated by the terminal transferase reaction (see below). Thus, K_m and k_{cat} for ATP represent composite values of both TNT- and template-dependent reactions.

NS5B Can Extend the RNA Chain after RMP Incorporation. We next tested whether incorporation of RMP would interfere with the subsequent incorporation of normal NMP during RNA synthesis. Using the 62-nucleotide template and [γ-^{32}P]GGA primer, NS5B produced a GGAG RNA product when provided with GTP (Figure 5, lane 3), and GGAG plus GGAGU when provided with GTP and a chain terminator nucleotide 3′-dUTP (lane 7). These products comigrated with the control RNAs made by T7 RNA polymerase (lanes 4 and 8) using the corresponding T7-DNA templates. Similar products were obtained when GTP was replaced with RTP (lanes 2 and 6) with one notable exception; the absence of the GGAR in lane 6 suggests that NS5B was able to extend all its GGAR product to GGARU.

These results indicate that NS5B is able to extend its RNA chain at least one nucleotide after it had incorporated an RMP residue. This begged the question of whether NS5B could incorporate multiple RMPs. When GTP was completely replaced with RTP in the reaction mixture, the full-length 62-nucleotide RNA product was made (Figure 5, lane 10), albeit at a much lower yield than when GTP was used (lane 11). Multiple truncated RNA products were also produced, primarily smaller in size (lane 10). Together, these data suggest that NS5B can incorporate RMP and extend its RNA chain, but does so at an impaired efficiency.

Multiple-RMP Incorporation Induced the Formation of Stalled Intermediate Complexes. During the elongation phase of transcription, DNA-dependent RNA polymerases may pause, arrest, or dissociate from the DNA template (*31*, *32*). Paused complexes slowly but eventually read through the pausing sites. Arrested complexes, in contrast, become permanently stuck unless the presence of certain protein factors intervenes (*31*, *32*). To test whether the truncated RNAs made in the presence of RTP can be chased into the full-length product, we first incubated the reaction mixture containing ATP, UTP, CTP, and RTP for 30 min (Figure 6A, lane 3), and then added back GTP for an additional 30

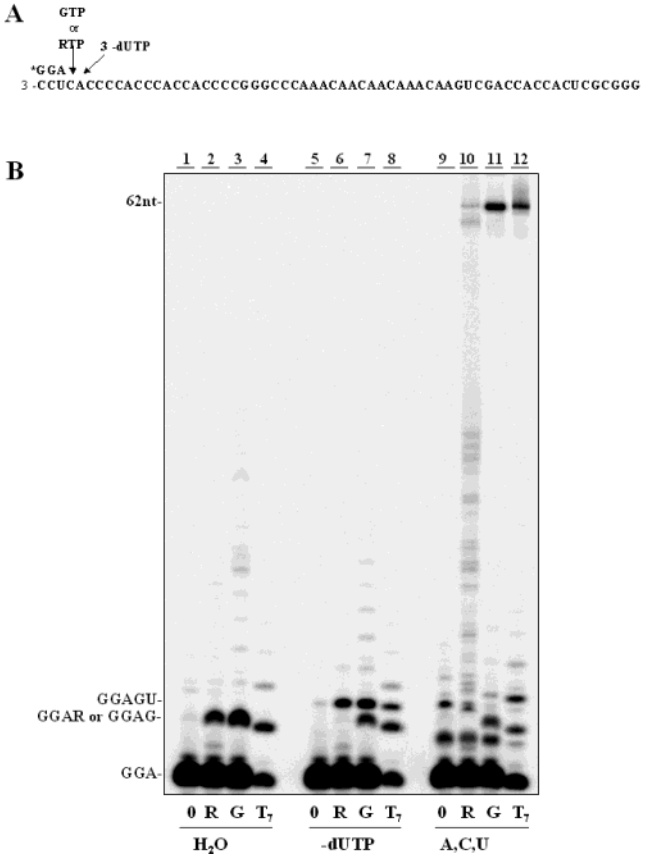

FIGURE 5: Extension of the RNA chain following RMP incorporation. (A) Experimental scheme showing the 62-nucleotide template and primer GGA for the limited nucleotide incorporation assay. A single RTP or GTP without other NTPs (lanes 1−4), with 3′-dUTP (lanes 5−8), or with ATP, CTP, and UTP (lanes 9−12) was used in the reactions. The same RNA made by T7 RNA polymerase from a DNA template were included as a marker (lanes 4, 8, and 12).

min incubation (lane 4). Most of the truncated RNAs were chased to the full-length RNA product. However, a small fraction, especially the 5−10-nucleotide RNAs, could not be chased with GTP, suggesting that either these complexes were arrested or the RNA has dissociated from the template (Figure 6A, compare lanes 3 and 4). To eliminate the possibility that NS5B might have been inactivated over time, we included a control in which the enzyme was incubated with the primer, template, and ATP, UTP, and CTP (no RTP or GTP), and after a 30 min incubation, GTP was added. The full-length RNA was produced, indicating that HCV polymerase is stable under this reaction condition (lanes 1 and 2).

When GTP was present together with RTP, the paused elongation intermediates were not detected when the GTP:RTP ratio was 1:50 or higher (Figure 6B, lanes 9−11). Since GTP was incorporated much more efficiently than RTP, these data suggest that the incorporation of multiple RMPs is necessary to cause transcriptional blockage. As noted earlier, the RMP-induced blockage occurred within a specific region near the 3′ end of the template that was used. To investigate this in detail, we performed RNase cleavage analysis on the RNA product (Figure 6B, lanes 1−7). By comparing RNase A and RNase T1 digest patterns of the 5′-end-labeled RNA product (Figure 6B, lanes 5 and 6) with the RMP-induced truncated RNAs (Figure 6B, lanes 7 and 8), we determined

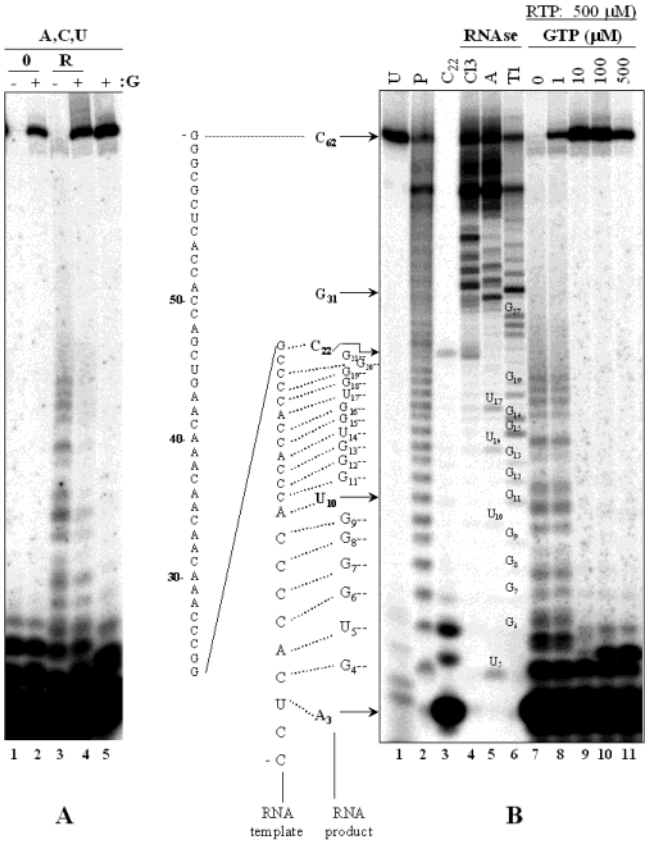

FIGURE 6: Characterization of the stalled elongation intermediates induced by RTP. (A) Extension of stalled elongation intermediates by the addition of GTP. RNA synthesis was performed using 0.1 mM ATP, CTP, and UTP in the absence (lanes 1 and 2) or presence (lanes 3 and 4) of 0.5 mM RTP at 30 °C for 1 h, followed by the addition of 0.1 mM GTP (lanes 2 and 4). All four reaction mixtures were incubated for an additional 1 h. Synthesis in the presence of all four NTPs without RTP at 30 °C for 2 h was included as a positive control (lane 5). (B) Characterization of the stalled elongation complexes. RNA synthesis was carried out in the presence of 0.5 mM RTP and 0.1 mM ATP, CTP, and UTP in the absence of GTP (lane 7) or in the presence of increasing concentrations of GTP (lanes 8−11). The sizes of elongation intermediates were aligned with the sequences of the template and predicted RNA product. The sequence of the 62-nucleotide RNA product was analyzed by partial digestion of the 5′-end-labeled RNA with RNase Cl3 (lane 4), A (lane 5), and T1 (lane 6). RNase Cl3 specifically cuts 3′ of C residues; A cuts 3′ of C and U residues, and T1 cuts 3′ of G residues: lane 1, untreated RNA; lane 2, piperidine ladder; and lane 3, a 22-nucleotide RNA product as a marker synthesized from a DNA template by T7 RNA polymerase.

that RMP causes RNA synthesis to stall primarily before the G27 position of the template. Intriguingly, this region contains many consecutive C residues, which can serve as template sites for RMP incorporation. The remaining sequence on the template contained very few consecutive C residues; correspondingly, very few stalled intermediates were detected in this region. Altogether, our data suggest that incorporation of multiple consecutive RMPs caused transcriptional blockage.

RNA Synthesis Using an RNA Template Containing a Ribavirin Residue. We next examined whether an RNA containing RMP can serve as a template for HCV NS5B. We used the Rib10 template, a 10-nucleotide RNA fragment derived from the 3′ end of the 62-nucleotide template, which harbors a ribavirin, instead of a C, at the fourth position (Figure 7, top). The SNI assay using the GGA primer revealed that CTP and UTP could be incorporated across from R, with CTP (Figure 7, lanes 12−14) being more efficient than UTP (lanes 17−19). Neither GTP (Figure 7, lanes 7−9) nor RTP (lanes 22−24) could be incorporated across from R. Since ATP was incorporated even in the absence of the template (Figure 7, lanes 5 and 6), its template-specific incorporation could not be evaluated under this condition.

To test whether ATP can be added across from R, we further performed an RdRP assay based on *de novo* synthesis using [γ-^{32}P]GTP (Figure 8A, top). GTP alone produced a GG dinucleotide product (lane 2), and GTP and ATP produced GG and GGA products; no products longer than three nucleotides were detected (lane 3). The synthesis of RNA products with at least eight nucleotides required either CTP (lane 4), UTP (lane 5), or both (lane 6) in addition to GTP and ATP; however, the efficiency of their production was very low, indicating that RNA synthesis across R is inefficient. The slowly migrating products ~20 nucleotides in length (lanes 4−6) near the control G_{21} RNA (lane 7) are most likely RNA duplexes of the template (10 nucleotides) and full-length products (8−10 nucleotides) that were not completely denatured in 8 M urea−PAGE. Thus, NS5B requires incorporation of CMP or UMP (but not AMP or GMP) opposite R on the template to read through this site. Overall, the ribavirin-containing RNA is a poor template. This was particularly evident when the amount of full-length products made from the Rib10 template was compared with the amount of the TG10 template, whose sequence is identical to that of Rib10 except for the replacement of G for R at the fourth position from the 3′ end of the template (Figure 8B, lanes 1−4 *vs* lanes 5−8). The level of full-length synthesis from the TG10 template is 10−35-fold higher than that from Rib10 at 1−1000 μM CTP tested. The level of full-length synthesis from the original 62-nucleotide RNA template (Figure 8B, lanes 9−12) was ~400 times higher than that from Rib10, suggesting that the length of the template can influence the RdRp activity of NS5B.

Kinetic analysis revealed that incorporation of R-templated CMP or UMP was much slower than the corresponding incorporation of RMP across from G or A, respectively (Table 1). The k_{cat}/K_m parameter shows that R-templated UTP incorporation is ~3000-fold catalytically less efficient than A-templated UTP incorporation (Table 2). R-Templated CTP incorporation was 4 times more efficient than R-templated UTP incorporation, but was still ~200-fold less efficient than G-templated CTP incorporation. However, HCV polymerase incorporated CTP and UTP across from R at similar efficiencies when these nucleotides were present at high concentrations (data not shown). These results confirmed ribavirin as a purine analogue that behaves with a bias toward being a more G-like than A-like analogue. Incorporation of C and U across from an R residue would lead to mutagenesis of RNA. Reduction of the level of full-length RNA synthesis from a ribavirin-containing RNA template revealed yet another facet of the effect of ribavirin on HCV NS5B-mediated RNA synthesis.

DISCUSSION

The important role of ribavirin in combating HCV infection is indicated by the fact that a combination of interferon-α

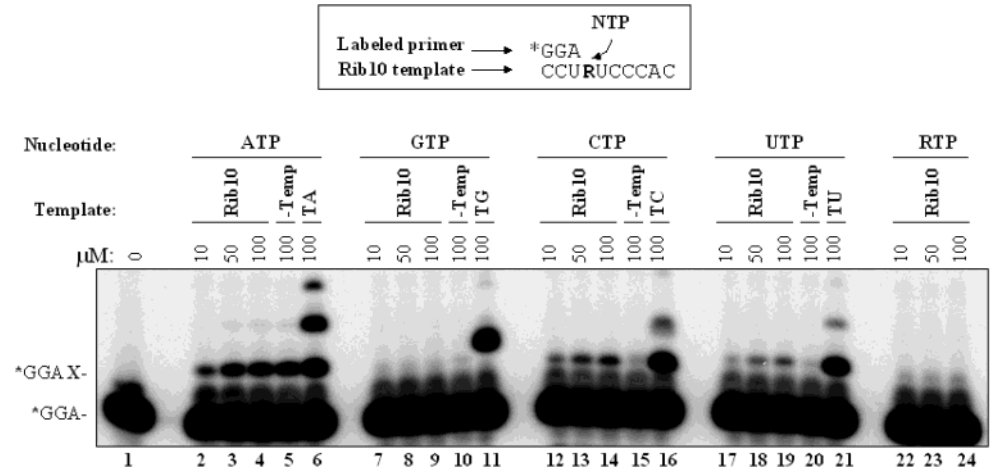

FIGURE 7: NS5B-mediated RNA synthesis from an RNA template containing a ribavirin residue. (Top) RNA primer and template used in this assay. (Bottom) The Rib10 RNA template contained a ribavirin residue at the fourth position from the 3′ end. Each reaction mixture contained a single NTP at a concentration 0, 50, or 100 μM. −Temp means no template (lanes 5, 10, 15, and 20). TA, TG, TC, and TU are 62-nucleotide template variants containing different nucleosides, instead of ribavirin, at the fourth position.

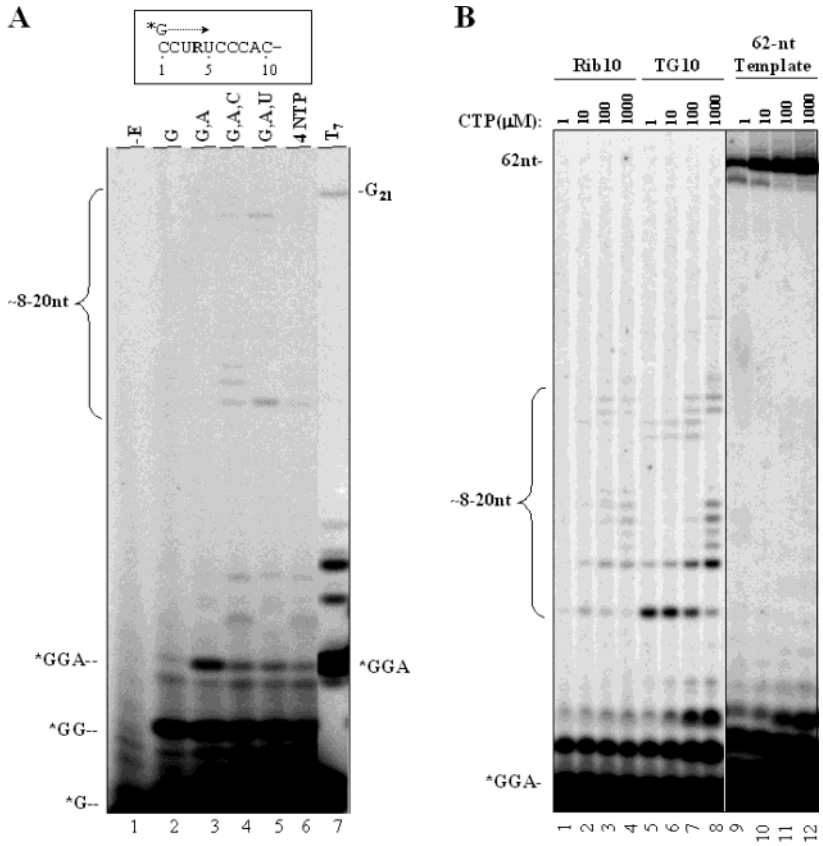

FIGURE 8: NTP requirement for full-length RNA synthesis on the ribavirin-containing template. (A) *De novo* RNA synthesis assay using [γ-^{32}P]GTP and the Rib10 RNA template (top). The NTPs present in the reaction mixture are indicated at the top of each lane. −E means no enzyme (lane 1). (B) *De novo* RNA synthesis using the Rib10 template (lanes 1−4), TG10 (lanes 5−8), or the 62-nucleotide template (lanes 9−12). TG10 is identical to Rib10 except that R is replaced with G. Each reaction mixture contained increasing concentrations (from 1 to 1000 μM) of CTP and each of the remaining three NTPs at 0.1 mM.

and ribavirin results in significantly more viral clearance in patients than that with interferon-α alone. The traditional view that ribavirin mediates its antiviral action through inhibition of IMPDH has been challenged by recent studies of the effect of ribavirin on poliovirus by Crotty and colleagues, which showed that ribavirin is promiscuously incorporated as a GTP or ATP analogue to create transition mutations in the RNA (*1*). Our results presented here also demonstrate that HCV polymerase uses RTP as a triphosphate analogue of purine but not pyrimidine and, conversely, ribavirin serves as a template residue for the incorporation of only pyrimidine but not purine nucleotides. The combination of these actions will result in a weak mutagenic effect. Furthermore, the efficiency of RMP incorporation is low, as compared to that of GMP or AMP, and RNA containing RMP is a poor template for HCV polymerase. Thus, a weak mutagenic effect and an inhibitory effect on HCV RNA synthesis may account for the antiviral activity of ribavirin. Intriguingly, we found that T7 DNA-dependent RNA polymerase (DdRP) could not use RTP as a GTP substitute.

Additional RMP incorporation studies with different viral RdRPs as well as other DdRPs, particularly those of mammalian origin, are needed to verify whether RMP incorporation is specific only for certain viral RdRPs.

Incorporation of RTP by HCV Polymerase Is Template-Specific but Catalytically Inefficient Compared to Normal NTP Incorporation. Using carboxy-terminally truncated NS5B and heteropolymeric RNA template, K_m values of 1−3 μM for GTP and ATP have been reported from *in vitro* assays (*33*). Our single-nucleotide incorporation assay using full-length NS5B yielded K_m values in the range of 4−5 μM for GTP and ATP, as compared to a value of ∼100 μM for RTP. Comparison of the k_{cat}/K_m ratio, a measure of the catalytic efficiency and enzyme specificity for a nucleotide substrate, revealed that HCV polymerase incorporates RMP 50−100-fold less efficiently than normal NMP. Using an HCV polymerase derivative lacking the β-loop and a 21-amino acid C-terminus (NS5B-BLΔ8), Maag *et al*. found a catalytic efficiency of RMP incorporation lower (∼7000-fold) than that of natural NMP incorporation (*26*). Incorporation of RMP by poliovirus RNA polymerase is ∼190000-fold less efficient than the incorporation of normal NMP (*1*). The large differences in these reported RMP incorporation efficiencies might be due to the different polymerases and reaction conditions that were employed. Polymerases such as *E. coli* DdRP exhibit apparent K_m values which vary by a factor of up to 1000 for different positions in the template (*34*). Thus, the relative efficiencies of incorporation of NMP and RMP by viral RdRPs may also vary significantly from one template position to the next. As a result, the overall efficiency of RMP incorporation is low and depends on the relative concentration of RTP and NTP in the cells.

We found RMP incorporation opposite C is ∼3 times more efficient catalytically than that opposite U. The efficiency of incorporation of CTP opposite R is 4-fold higher than that of incorporation of UTP opposite R. These findings suggest RTP is more of a GTP mimic than ATP in the HCV replicase system. A higher RMP incorporation efficiency opposite C than opposite U would theoretically lead to the more frequent occurrence of A to G or U to C transition mutations than the reverse. Indeed, Contreras and co-workers reported that ribavirin treatment of HepG2 cells harboring a DNA-based binary HCV expression system led to a higher frequency of A to G mutations than G to A and a higher frequency of U to C mutations than C to U (*24*). Confirmation of these types of mutations awaits further *in vivo* studies. Contrary to our findings, studies using the HCV polymerase NS5B-BLΔ8 (*26*) and poliovirus RNA polymerase (*1*) reported equal catalytic efficiencies of incorporation of RMP opposite C or U template site. Whether the nature of RNA polymerases and/or templates used in the assay caused these differences will need further investigation.

Inhibitory Effects of Ribavirin Triphosphate on RNA Synthesis by HCV RNA Polymerase. In the absence or presence of a very low GTP concentration, RTP severely inhibits productive full-length RNA synthesis. The inhibition appears to be due to the formation of stalled elongation complexes resulting from multiple-RMP incorporation. The incorporated RMP did not act as an RNA chain terminator since the stalled complexes can be chased to full-length RNA upon addition of GTP. Thus, RMP-mediated inhibition is different from that of a classical chain terminator such as 3TCTP or FTCTP, each of which is a nucleoside analogue lacking the 3′-OH group on the ribose ring, which is incorporated into RNA products by HIV-1 RT and causes DNA chain termination (*35*). It is unclear why multiple-RMP incorporation causes HCV polymerase to stall. It is conceivable that ribavirin incorporation perturbs the structure at the 3′ end of the RNA product, resulting in a structural conformation that is unfavorable for template pairing or interaction with the active center of the HCV polymerase.

Ribavirin triphosphate, however, has only a minor inhibitory effect on RNA synthesis when NTP is abundant. The presence of ≤2 mM RTP and ≤0.1 mM normal NTP resulted in only a slight reduction the level of RNA synthesis (Figure 2). Such inhibition could be due to an allosteric effect, as in the case of certain derivatized phenylalanine compounds recently reported to bind to an allosteric site away from the HCV polymerase's catalytic center (*36*). However, an allosteric effect is unlikely to be the cause of the RTP-mediated inhibition since we found that RTP competitively inhibited incorporation of GMP but not UMP. Instead, our results suggest that the inhibition is due to interference with incorporation of purine by RTP. The inhibition is minor because at 100 μM NTP, a concentration well above the K_m values of GTP (4.9 μM) and ATP (4.4 μM), RTP is probably not an effective substrate analogue competitor given its low catalytic incorporation efficiency. Weak inhibition is also consistent with the fact that RTP inhibits GMP incorporation with a K_i of 42 μM, a value much larger when compared to the K_m of 4.9 μM for GTP. This is in contrast with the potent competitive inhibition of IMPDH by RMP, with a reported K_i of 0.25 μM as compared to the K_m of 18 μM for its natural substrate. These, along with the fact that RMP incorporation does not lead to RNA chain termination, explain why significant inhibition is observed only at very low GTP concentrations.

Effects of Ribavirin Incorporation on the Template Activity of RNA. A drastic reduction in the level of HCV NS5B-mediated RNA synthesis was observed when an RNA template containing a ribavirin residue was used. This could be explained in part by the large increase in the K_m values of pyrimidine triphosphate at the R template site. For example, A-templated UTP incorporation gave a K_m of 0.6 μM, whereas the K_m for R-templated UTP incorporation is 76 μM, a 126-fold increase. Calculation of the catalytic efficiency, k_{cat}/K_m, revealed that R-templated UTP incorporation is ∼2800-fold less efficient than A-templated UTP incorporation, and that R-templated CTP incorporation is 230-fold less efficient than G-templated CTP incorporation. In fact, even at the saturating NTP concentration (1 mM), the efficiency of RNA synthesis from a normal RNA template is much higher (∼10−35-fold) than that from the ribavirin-containing template (Figure 8B, compare lanes 1−4 to lanes 5−8). Maag and co-workers also reported similar elongation impediment caused by the presence of a ribavirin residue in the template, but the effect was less drastic (2−4-fold) (*26*). Thus, ribavirin probably affects HCV RdRP most significantly during subsequent rounds of RNA synthesis after RMPs have been incorporated into the template.

In summary, our *in vitro* studies revealed that ribavirin has multiple effects on RNA synthesis by the HCV polymerase. Ribavirin likely causes a minor mutagenic effect by mimicking a purine nucleotide. It also suppresses RNA

synthesis at low GTP concentrations, a condition likely to be enhanced by the inhibition of IMPDH by RMP *in vivo*. Moreover, RMP incorporation creates RNAs that are poor templates for RNA synthesis by the HCV polymerase; this is due in part to the extremely low catalytic efficiency at the ribavirin site. These combined effects may account for the antiviral activity of ribavirin. The fact that ribavirin monotherapy fails to clear HCV infection suggests that HCV probably possesses its own mechanism for evading the ribavirin effect; illumination of such a mechanism will be vital to the development of effective therapeutic drugs. Whether ribavirin and its three phosphate forms also affect other HCV enzymatic components, i.e., helicase, or processes such as translation remains to be studied. Nevertheless, the new role of ribavirin as a mutagen to HCV polymerase will motivate the development of mutagenic nucleoside analogues that are highly specific for this enzyme.

ACKNOWLEDGMENT

We thank Dr. Lilian Hsu of Mount Holyoke College (South Hadley, MA) and Jerry Tuler for critically reading the manuscript.

REFERENCES

1. Crotty, S., Maag, D., Arnold, J. J., Zhong, W., Lau, J. Y., Hong, Z., Andino, R., and Cameron, C. E. (2000) *Nat. Med. 6*, 1375−1379.
2. De Francesco, R. (1999) *J. Hepatol. 31*, 47−53.
3. Grakoui, A., Wychowski, C., Lin, C., Feinstone, S. M., and Rice, C. M. (1993) *J. Virol. 67*, 1385−1395.
4. O'Reilly, E. K., and Kao, C. C. (1998) *Virology 252*, 287−303.
5. Koonin, E. V. (1993) *Nucleic Acids Res. 21*, 2541−2547.
6. Behrens, S. E., Tomei, L., and De Francesco, R. (1996) *EMBO J. 15*, 12−22.
7. Lohmann, V., Korner, F., Herian, U., and Bartenschlager, R. (1997) *J. Virol. 71*, 8416−8428.
8. Oh, J. W., Ito, T., and Lai, M. M. (1999) *J. Virol. 73*, 7694−7702.
9. Cummings, K. J., Lee, S. M., West, E. S., Cid-Ruzafa, J., Fein, S. G., Aoki, Y., Sulkowski, M. S., and Goodman, S. N. (2001) *JAMA, J. Am. Med. Assoc. 285*, 193−199.
10. Davis, G. L., Esteban-Mur, R., Rustgi, V., Hoefs, J., Gordon, S. C., Trepo, C., Shiffman, M. L., Zeuzem, S., Craxi, A., Ling, M. H., and Albrecht, J. (1998) *N. Engl. J. Med. 339*, 1493−1499.
11. Sidwell, R. W., Huffman, J. H., Khare, G. P., Allen, L. B., Witkowski, J. T., and Robins, R. K. (1972) *Science 177*, 705−706.
12. McCormick, J. B., King, I. J., Webb, P. A., Scribner, C. L., Craven, R. B., Johnson, K. M., Elliott, L. H., and Belmont-Williams, R. (1986) *N. Engl. J. Med. 314*, 20−26.
13. Hall, C. B., Walsh, E. E., Hruska, J. F., Betts, R. F., and Hall, W. J. (1983) *JAMA, J. Am. Med. Assoc. 249*, 2666−2670.
14. Groothuis, J. R., Woodin, K. A., Katz, R., Robertson, A. D., McBride, J. T., Hall, C. B., McWilliams, B. C., and Lauer, B. A. (1990) *J. Pediatr. 117*, 792−798.
15. Miller, J. P., Kigwana, L. J., Streeter, D. G., Robins, R. K., Simon, L. N., and Roboz, J. (1977) *Ann. N.Y. Acad. Sci. 284*, 211−229.
16. Streeter, D. G., Miller, J. P., Robins, R. K., and Simon, L. N. (1977) *Ann. N.Y. Acad. Sci. 284*, 201−210.
17. Streeter, D. G., Witkowski, J. T., Khare, G. P., Sidwell, R. W., Bauer, R. J., Robins, R. K., and Simon, L. N. (1973) *Proc. Natl. Acad. Sci. U.S.A. 70*, 1174−1178.
18. Crotty, S., Cameron, C., and Andino, R. (2002) *J. Mol. Med. 80*, 86−95.
19. Lanford, R. E., Chavez, D., Guerra, B., Lau, J. Y., Hong, Z., Brasky, K. M., and Beames, B. (2001) *J. Virol. 75*, 8074−8081.
20. Wray, S. K., Gilbert, B. E., Noall, M. W., and Knight, V. (1985) *Antiviral Res. 5*, 29−37.
21. Goswami, B. B., Borek, E., Sharma, O. K., Fujitaki, J., and Smith, R. A. (1979) *Biochem. Biophys. Res. Commun. 89*, 830−836.
22. Cassidy, L. F., and Patterson, J. L. (1989) *Antimicrob. Agents Chemother. 33*, 2009−2011.
23. Crotty, S., Cameron, C. E., and Andino, R. (2001) *Proc. Natl. Acad. Sci. U.S.A. 98*, 6895−6900.
24. Contreras, A. M., Hiasa, Y., He, W., Terella, A., Schmidt, E. V., and Chung, R. T. (2002) *J. Virol. 76*, 8505−8517.
25. Severson, W. E., Schmaljohn, C. S., Javadian, A., and Jonsson, C. B. (2003) *J. Virol. 77*, 481−488.
26. Maag, D., Castro, C., Hong, Z., and Cameron, C. E. (2001) *J. Biol. Chem. 276*, 46094−46098.
27. Ranjith-Kumar, C. T., Gajewski, J., Gutshall, L., Maley, D., Sarisky, R. T., and Kao, C. C. (2001) *J. Virol. 75*, 8615−8623.
28. Vo, N. V., Oh, J. W., and Lai, M. M. (2003) *Virology 307*, 301−316.
29. Kubori, T., and Shimamoto, N. (1996) *J. Mol. Biol. 256*, 449−457.
30. Vo, N. V., Hsu, L. M., Kane, C. M., and Chamberlin, M. J. (2003) *Biochemistry 42*, 3787−3797.
31. Arndt, K. M., and Chamberlin, M. J. (1990) *J. Mol. Biol. 213*, 79−108.
32. Uptain, S. M., Kane, C. M., and Chamberlin, M. J. (1997) *Annu. Rev. Biochem. 66*, 117−172.
33. Carroll, S. S., Sardana, V., Yang, Z., Jacobs, A. R., Mizenko, C., Hall, D., Hill, L., Zugay-Murphy, J., and Kuo, L. C. (2000) *Biochemistry 39*, 8243−8249.
34. Levin, J. R., and Chamberlin, M. J. (1987) *J. Mol. Biol. 196*, 61−84.
35. Gao, H. Q., Boyer, P. L., Sarafianos, S. G., Arnold, E., and Hughes, S. H. (2000) *J. Mol. Biol. 300*, 403−418.
36. Wang, M., Ng, K. K., Cherney, M. M., Chan, L., Yannopoulos, C. G., Bedard, J., Morin, N., Nguyen-Ba, N., Alaoui-Ismaili, M. H., Bethell, R. C., and James, M. N. (2003) *J. Biol. Chem. 278*, 9489−9495.

BI0344681